

**INTERPLAY BETWEEN N···H, N···X AND  $\pi$ ···X INTERACTIONS IN THE COMPLEX PAIRING OF PYRAZINE WITH HYPOHALOUS ACIDS: A NBO AND QTAIM (QUANTUM THEORY OF ATOMS IN MOLECULES) ANALYSIS**

Abedien Zabardasti<sup>1\*</sup>, Yunes Abbasi Tyula<sup>1</sup> and Hamid Goudarziafshar<sup>2</sup>

<sup>1</sup>Department of Chemistry, Lorestan University, Khorramabad, Iran

<sup>2</sup>Department of Chemistry, Faculty of Science, Sayyed Jamaledinasadabadi University, Asadabad, Iran

(Received January 24, 2016; revised July 23, 2017)

**ABSTRACT.** The theoretical calculations of the complexes formed by pyrazine (PZ) with hypohalous acids (HOX; X= F, Cl, Br and I) have been carried out at the MP2/6-311++G(2d,2p) computational level. PZ and HOX molecules could have three different types of interactions including hydrogen bond (N···H) and halogen bonds (N···X,  $\pi$ ···X). The nature of halogen atom has a small effect on the hydrogen bonds, whereas it imposes a great impact on the halogen bond interactions. The strength, properties and nature of interactions were analyzed using natural bond orbital (NBO) and atoms in molecules (AIM) theories.

**KEY WORDS:** Pyrazine, Hypohalous acid, Hydrogen bonding, Halogen bonding,  $\pi$ ···X interaction

## INTRODUCTION

Noncovalent interactions play an extensive and important role in drug optimization, supramolecular assembly, crystal engineering, reaction selectivity and molecular biology [1-4]. Undoubtedly, hydrogen bond (HB) is still one of the most important intermolecular interactions and its formation is mainly due to the electrostatic interaction, together with the induction and dispersion interactions [5, 6].

Recently, a growing amount of experimental and theoretical evidence has demonstrated that halogen bonds (XB) interactions play a key role in a wide variety of chemical systems such as biochemistry and medicinal chemistry [7-9]. Because they are often involved in protein-ligand interactions that are either biologically detrimental, as in the case of interactions involving organohalogens found in the environment, or beneficial because of their potential usefulness in the design of novel ligands that interact with proteins in a very specific way [10, 11]. Extensive studies have shown that many properties of the halogen bond are analogous to those of the hydrogen bond [12-14]. For example, concerning strength, halogen bonds are comparable to hydrogen bonds and thus a competition may occur between them, thus in recent years much attention has been paid to it [9, 15-17].

Hypohalous acids (HOX, where X is F, Cl, Br, and I) are a very interesting class of compounds because their structure allows them to participate in both HB and XB interactions [18-22]. Both types of interactions are of importance for the understanding of the above chemical and biological processes. More importantly, they provide a good model to study the competition between HB and XB [19, 23-25]. In general, the HB complexes are more stable for HOCl and HOBr while the XB isomers are more stable for HOI. These compounds play an important role both in atmospheric chemistry involved in catalytic cycles in the seasonal depletion of the ozone layer in the stratosphere [26-28] and pathophysiological processes [29]. HOXs are unstable and readily form OX radicals in the atmosphere and they appear as reservoirs and sinks of OX radicals in atmospheric chemistry [28]. Thus, the chemical instability

\*Corresponding author. E-mail: zebardasti@yahoo.com

This work is licensed under the Creative Commons Attribution 4.0 International License

of HOXs makes it difficult to experimentally study their properties. The HOXs are only stable in solution, only hypofluorous acid (HOF) was obtained pure in the condensed phase where X-ray analysis revealed the infinite angular O–H—O chains [30]. In addition, they, as powerful oxidizing agents can participate in oxidation, epoxidation and hydroxylation processes [31, 32]. The HOXs present lower acidities than hydrohalic acids HX (X = F, Cl, Br, and I); however, they are more acidic than water [33]. A number of studies have characterized the hydrogen bonded cluster formed by the HOXs with themselves [34-36] or with other molecules [18, 21, 37-39]. The structures, properties and interaction nature in these complexes have been understood with the natural bond orbital (NBO) and atoms in molecules (AIM) theories.

On the other hand, pyrazine (hereafter, denoted as PZ) is a heterocyclic aromatic organic compound with the chemical formula  $C_4H_4N_2$ . PZ is a symmetrical molecule with point group  $D_{2h}$ , its derivatives such as phenazine are well known for their antitumor, antibiotic and diuretic activities [40]. To the best of our knowledge, neither theoretical nor experimental data regarding the structural information of the interaction of PZ with any of the HOXs is available in the literature. In the absence of experimental information, a theoretical analysis of the existence of such complexes and their properties appear to be in order. The present work reports a detailed examination of the stabilities, electronic structure, and vibrational frequencies of these complexes.

### COMPUTATIONAL METHODS

Geometry optimizations of the monomers and complexes were performed at the MP2 method [41] with the 6-311++G(2d,2p) [42] basis set for all atoms, except iodine, for which the def2-TZVPP [43] basis set was used. Harmonic vibrational frequency calculations were used at the same level of theory to identify the local minima structures on the potential energy surfaces and to obtain zero-point vibrational energy (ZPVE). The interaction energy ( $\Delta E$ ) was calculated as the difference between the total energy of the complex and the sum of total energies of the monomers. The basis set superposition error (BSSE) was estimated with the counterpoise (CP) method of Boys and Bernardi [44] to correct the interaction energy. The natural bond orbital (NBO) method [45] was used to analyze the interaction of the occupied and empty orbitals via procedures contained within Gaussian 03 [46]. The electron density topological analysis based on the theory of atoms in molecules (AIM) for all the complexes were performed at the MP2/6-311++G(2d,2p) computational level using the AIM2000 program [47]. All calculations were carried out using the Gaussian 03 package [46].

### RESULTS AND DISCUSSION

The results of geometry optimizations (stabilization energies, binding distances, vibrational stretching frequencies and structures) for the PZ and its complexes with HOX (X = F, Cl, Br and I) molecules are given in Tables 1–4 and Figure 1. Regarding the methods of electron donation from PZ to HOX, two models interactions were considered.

The first is PZ:HOX-A in which PZ could have either hydrogen bond (PZ:HOX-A-HB) or halogen bond (PZ:HOX-A-XB) interactions with HOX molecules, Figure 1. For the second one (PZ:HOX-B) we could only optimize the XB interactions. In model A, interactions were carried out using N electron lone pairs of PZ, but in the model B  $\pi$ -electrons of PZ roles out as electron donor. The binding distance, hydrogen and halogen bond angle of respective complexes, and changes in the O-H and O-X bond lengths are given in Table 2. The  $N\cdots H$ ,  $N\cdots X$  and  $\pi\cdots X$  distances are in the ranges of 1.752–1.769 Å, 2.519–3.021 Å and 3.100– 3.182 Å, respectively. The given values are smaller than the sum of the van der Waals radii of the respective atoms (2.6 Å for H and N atoms, 2.9 Å for F and N atoms, 3.3 Å for Cl and N atoms, 3.5 Å for Br and N atoms, 3.6 Å for I and N atoms, 3.5 for C and Cl atoms, 3.6 for C and Br, 3.8 for C and I).

The  $H\cdots F$  distance almost amounts to the sum of the van der Waals radii of the H and F atoms (2.5 Å for H and F atoms). This confirms the presence of the  $H\cdots N$  hydrogen bond in PZ:HOX-A-HB ( $X = F, Cl, Br, I$ ); and also the  $X\cdots N$  ( $X = F, Cl, Br, I$ ) and the  $X\cdots\pi$  ( $X = Cl, Br, I$ ) halogen bond interactions in the PZ:HOX-A-XB and PZ:HOX-B complexes, respectively. For the HOF only the PZ:HOF-A structures could be optimized. The interaction energy is a convincing measurement for the stability of studied complexes.

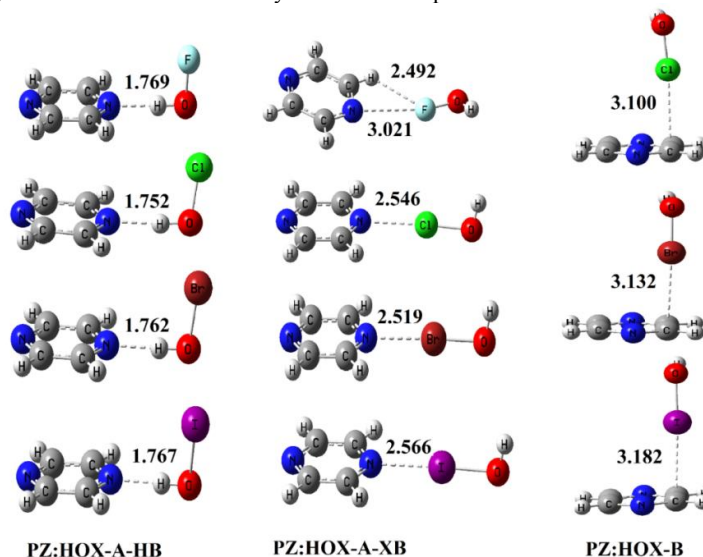


Figure 1. Optimized structures of the complexes between PZ-HOX ( $X = F, Cl, Br$  and  $I$ ) at the MP2/6-311++G(2d,2p) computational level.

According to the interaction energies (Table 1), the stabilities of PZ:HOX-A-HB ( $X = F, Cl, Br$ ) complexes are greater than PZ:HOX-A-XB and PZ:HOX-B, but in the case of  $X = I$  the PZ:HOI-A-XB is more stable than PZ:HOI-A-HB and PZ:HOI-B. Hydrogen bonding in PZ:HOX-A-HB complexes were not influenced by X atom, considerably, thus their stabilization energies are close together. The  $H\cdots N$  distance in PZ:HOF-A-HB is longer than other PZ:HOX-A-HB ( $X = Cl, Br$  and  $I$ ) complexes. It is in line with its stability and this subject has been demonstrated in the HB complexes of hypohalous acids previously [39, 48]. This might be attributed to the nature of O–X bonds, since O–F bond is a covalent, polarized bond, while other O–X bonds are of electron donor–acceptor-type with the halogen donating electron density to the valence shell of oxygen [19, 49]. There is a good linear correlation coefficient between the change of the  $H\cdots N$  distance and interaction energy ( $SE^{corr}$ ) in PZ:HOX-A-HB complexes (Figure 2).

However, in the XB complexes, with an increase in the mass of halogen, there is an increase in both the electron density at the bond critical point and stabilization energy. According to the concept of  $\sigma$ -hole (the region of the positive potential on the outermost region of a halogen's surface) which is used to explain the halogen bonding, a halogen atom with positive  $\sigma$ -hole interacts more effectively with the sites rich in electron. Therefore, a halogen atom with more positive  $\sigma$ -hole forms a stronger halogen bond interaction. Since Br has a larger atomic radius than that of Cl, the effective nuclear charge of Br on valence electrons decreases and its  $\sigma$ -hole becomes stronger and more positive. As a result, the halogen bonding of Br and its complex

become stronger and more stable than those of Cl. The same is true for iodine and bromine. Thus, the strength of the XB increases as follows:  $F < Cl < Br < I$ , and iodine forms the strongest XB (Table 1). This trend also could be related to the role of atomic quadrupoles ( $\Theta_{zz}$ ) on the halogen atoms in the XB complexes [50]. The quadrupole of the halogen atoms increases in the order of  $F < Cl < Br < I$ . Thus stabilities of XB complexes are in agreement with the sequence given for  $\Theta_{zz}$  of the halogen atoms, Figure 3. Regarding Table 2, the H–O bond is elongated in PZ:HOX-A-HB, shortened in the PZ:HOX-A-XB except in PZ:HOF-A-HB and remained constant in the PZ:HOX-B. The X–O bond is lengthened in XB complexes and contracted in HB ones except in PZ:HOF-A-HB which it shows a small elongation. Table 3 presents stretching frequencies of HOX as well as the H–O and O–X band shifts. In the free HOX molecules the stretching frequencies of the H–O and X–O bonds were appeared around 3797–3806 and 590–954  $\text{cm}^{-1}$ , respectively.

Table 1. Uncorrected stabilization energy ( $SE^{\text{uncorr.}}$ ), BSSE and stabilization energy corrected with BSSE and  $\Delta ZPE$  ( $SE^{\text{corr.}}$ )<sup>a</sup> all in  $\text{kcal mol}^{-1}$  at the MP2/6-311++G(2d,2p) level<sup>b</sup>.

Complex	$SE^{\text{uncorr.}}$	$\Delta ZPE$	BSSE	$SE^{\text{corr.}}$
PZ:HOF-A-HB	-10.78	1.60	1.91	-7.27
PZ:HOCl-A-HB	-11.24	1.55	2.12	-7.57
PZ:HOBBr-A-HB	-10.94	1.51	2.07	-7.36
PZ:HOI-A-HB	-11.12	1.44	2.33	-7.35
PZ:HOF-A-XB	-1.67	0.41	0.62	-0.64
PZ:HOCl-A-XB	-6.19	0.78	1.88	-3.53
PZ:HOBBr-A-XB	-9.22	0.80	2.02	-6.4
PZ:HOI-A-XB	-12.95	0.84	2.98	-9.13
PZ:HOCl-B	-3.19	0.37	1.23	-1.59
PZ:HOBBr-B	-3.82	0.38	1.56	-1.88
PZ:HOI-B	-5.54	0.35	2.41	-2.78

<sup>a</sup> $SE^{\text{cor}}$

<sup>b</sup> $r = SE^{\text{uncorr.}} + BSSE + \Delta ZPE$ . <sup>b</sup>For I atom, the def2-TZVPP pseudopotential basis set was adopted.

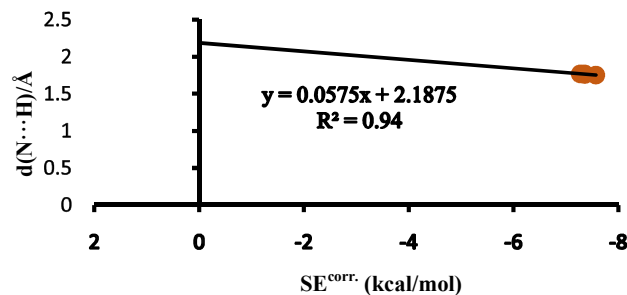
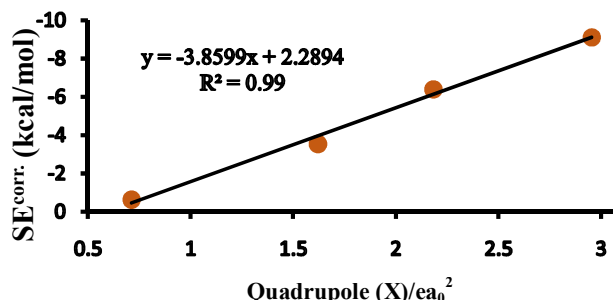


Figure 2. Plots of N...H distances versus interaction energies ( $SE^{\text{corr.}}$ ) in PZ:HOX-A-HB complexes.

Description of the HOX and PZ frequencies shift in HB versus XB complexation seems interesting. The O–X stretching frequencies show 5–11  $\text{cm}^{-1}$  blue shifts in PZ:HOX-A-HB but -9 to -68  $\text{cm}^{-1}$  red shifts in the PZ:HOX-A-XB complexes. On the other hand, in agreement with stabilities of adducts while blue shifts of O–X in the PZ:HOX-A-HB is not much sensitive to the X function but red shifts of this bond increased for heavier X atoms considerably.

Figure 3.  $SE^{corr.}$  versus quadrupole for PZ:HOX-A-XB complexes.Table 2. Binding distances ( $R/\text{\AA}$ ), bond lengths ( $r/\text{\AA}$ ) and their changes ( $\Delta r/\text{\AA}$ ), of respective complexes calculated at the MP2/6-311++G(2d,2p) level.

Compound	$R_1$	$R_2$	$r_{H-O}$	$\Delta r_{H-O}$	$r_{O-X}$	$\Delta r_{O-X}$	$\theta$
HOF	-	-	0.967	-	1.436	-	-
HOCl	-	-	0.966	-	1.719	-	-
HOBr	-	-	0.966	-	1.848	-	-
HOI	-	-	0.966	-	1.990	-	-
	N⋯H						
PZ:HOF-A-HB	1.769	-	0.990	0.023	1.442	0.006	171.3
PZ:HOCl-A-HB	1.752	-	0.991	0.025	1.713	-0.006	175.1
PZ:HOBr-A-HB	1.762	-	0.991	0.025	1.839	-0.009	178.1
PZ:HOI-A-HB	1.767	-	0.990	0.026	1.980	-0.010	174.0
	N⋯X		H⋯X				
PZ:HOF-A-XB	3.021	2.492	0.967	0	1.439	0.002	167.4
PZ:HOCl-A-XB	2.546	-	0.965	-0.001	1.746	0.028	177.5
PZ:HOBr-A-XB	2.519	-	0.965	-0.001	1.887	0.039	178.1
PZ:HOI-A-XB	2.566	-	0.964	-0.002	2.027	0.037	178.1
	C=C⋯X						
PZ:HOCl-B	3.100	-	0.966	0	1.725	0.006	168.1
PZ:HOBr-B	3.132	-	0.966	0	1.857	0.009	168.1
PZ:HOI-B	3.182	-	0.966	0	2.000	0.010	169.2

In contrast the H–O stretching frequencies displayed -479 to -525  $\text{cm}^{-1}$  red shifts in the PZ:HOX-A-HB but 10–19  $\text{cm}^{-1}$  blue shifts in the PZ:HOX-A-XB ( $X = \text{Cl}, \text{Br}, \text{I}$ ) complexes. In PZ:HOX-B small red shifts (-2 to -4  $\text{cm}^{-1}$  for H–O and -17 to -19  $\text{cm}^{-1}$  for O–X) were observed. The red shift of H–O in the PZ:HOX-B complexes can be due to the charge transfer of  $lp_X \rightarrow \pi^*_{C=C}$ , which leads to the decrease of the s-character in the oxygen hybrid orbital of the O–H bond, thus leading to the red shift of its stretching frequency. The N⋯H bands in PZ:HOX-A-HB appeared at 199–221  $\text{cm}^{-1}$  and it decreased with an increases in the mass of X atom. Also the N⋯X band in PZ:HOX-A-XB complexes observed in the range of 30–105  $\text{cm}^{-1}$  and it increased with an increases in the mass of X. There is a good linear relationship between the electron densities ( $\rho$ ) at the N⋯X BCPs with the  $\Delta r_{O-X}/\text{\AA}$  and  $\Delta v_{O-X}/\text{cm}^{-1}$  in the PZ:HOX-A-XB complexes (Figure 4).

Regarding the PZ:HOX-B, the stretching frequencies of their  $\pi \cdots X$  bonds are in the range of 76–84  $\text{cm}^{-1}$ . As shown in Table 4, the stretching frequencies of C=N ( $v_{C=N(\text{Sym})}$ ,  $v_{C=N(\text{Asym})}$ ) and C=C ( $v_{C=C}$ ) of PZ in the PZ:HOX-A-HB show blue shift (5–14  $\text{cm}^{-1}$ ) with complexation. It is clear that  $lp_N \rightarrow \sigma^*_{OH}$  intermolecular charge transfer decrease the intensity of  $lp_N \rightarrow \pi^*$

intramolecular transitions, so they lead to these blue shifts in PZ:HOX-A-HB complexes. In PZ:HOX-A-XB system the stretching frequencies of C=N and C=C bonds for X = F remained unchanged since no significant  $lp_N \rightarrow \sigma^*_{OF}$  charge transfer was occurred. But for X = Cl, Br, and I the  $lp_N \rightarrow \sigma^*_{OX}$  charge transfers leads to blue shift of C=N and C=C bonds (2–16  $\text{cm}^{-1}$ ) which this shift for  $\nu_{C=N(\text{Sym})}$  are greater than other ones. Eventually in PZ:HOX-B the  $\nu_{C=N(\text{Asym})}$  and  $\nu_{C=C}$  show small red shift while  $\nu_{C=N(\text{Sym})}$  shows blue shift with complexation. There is a good correlation between the  $\pi \cdots X$  distance with the stabilization energy ( $SE^{\text{corr}}$ ) and  $\Delta r_{O-X}/\text{\AA}$  in the PZ:HOX-B complexes (Tables 1, 2).

Table 3. Unscaled vibrational frequencies ( $\nu$ ,  $\text{cm}^{-1}$ ) with corresponding intensities (values given in parenthesis,  $\text{km mol}^{-1}$ ) and frequency shifts ( $\Delta\nu$ ,  $\text{cm}^{-1}$ ) of [PZ:HOX] complexes at the MP2/6-311++G(2d,2p) level.

Compound	$\nu_{\text{H-O}}$	$\Delta\nu_{\text{H-O}}$	$\nu_{\text{O-X}}$	$\Delta\nu_{\text{O-X}}$	$\nu_{\text{Y}\cdots\text{X}}$	$\nu_{\text{N}\cdots\text{H}}$
HOF	3797(49)	-	954(1)	-	-	-
HOCl	3803(83)	-	730(11)	-	-	-
HOBr	3801(92)	-	628(15)	-	-	-
HOI	3806(116)	-	590(23)	-	-	-
PZ:HOF-A-HB	3318(1435)	-479	959(4)	5	-	221(15)
PZ:HOCl-A-HB	3278(1670)	-525	739(9)	9	-	213(10)
PZ:HOBr-A-HB	3292(1702)	-509	643(12)	11	-	205(8)
PZ:HOI-A-HB	3294(1691)	-512	599(21)	9	-	199(8)
PZ:HOF-A-XB	3797(54)	0	945(0.38)	-9	30(8) <sup>a</sup>	-
PZ:HOCl-A-XB	3813(85)	10	664(112)	-66	93(12) <sup>a</sup>	-
PZ:HOBr-A-XB	3812(93)	11	560(120)	-68	98(16) <sup>a</sup>	-
PZ:HOI-A-XB	3825(109)	19	541(126)	-49	105(15) <sup>a</sup>	-
PZ:HOCl-B	3799(88)	-4	712(28)	-18	77(2) <sup>b</sup>	-
PZ:HOBr-B	3797(37)	-4	609(37)	-19	84(2) <sup>b</sup>	-
PZ:HOI-B	3804(133)	-2	573(51)	-17	76(1) <sup>b</sup>	-

<sup>a</sup>Y=N; <sup>b</sup>Y=C

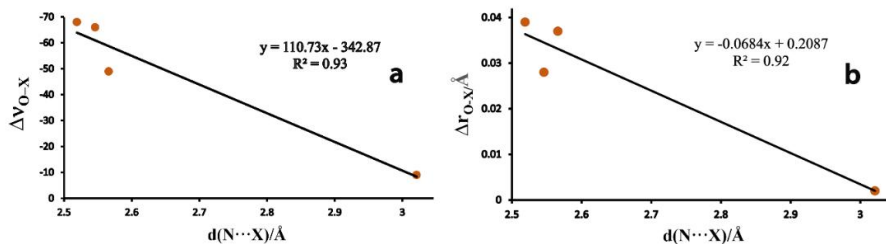


Figure 4. Relationship between the electron densities at the  $\text{N}\cdots\text{X}$  BCPs with the  $\Delta\nu_{\text{O-X}}$  (a) and  $\Delta r_{\text{O-X}}$  (b) in the PZ:HOX-A-XB complexes.

### AIM ANALYSIS

The atom in molecules (AIM) theory [47] was applied here to analyze the characteristics of the intermolecular bond critical points (BCP) in the studied complexes. The topological parameters including the electron density ( $\rho$ ), Laplacian of electron density at BCP ( $\nabla^2\rho_{\text{BCP}}$ ), and the energy density (Hc) at BCP which is the sum of the kinetic electron energy density ( $G_c$ ) and the potential electron density ( $V_c$ ), ( $H_c = G_c + V_c$ ), derived from the Bader theory also indicate the nature of interaction. The electron density ( $\rho$ ) had a positive correlation with bond strength, that

is, the  $\rho$  was bigger (smaller), and the bond strength was stronger (weaker). The  $\nabla^2\rho_{\text{BCP}}$  reflected the characters of bond, and the negative value of the Laplacian of the electron density at BCP ( $\nabla^2\rho_{\text{BCP}} < 0$ ) determined the concentration of the electron charge in the region between the nuclei of the interacting atoms and is typical of covalent bonds-shared interactions. In the case of the  $\nabla^2\rho_{\text{BCP}} > 0$ , there was a depletion of the electron charge between atoms, indicating that there is an interaction of closed-shell systems like ions, van der Waals interactions, or H-bonds. Therefore, when the  $\nabla^2\rho_{\text{BCP}} < 0$ , there was no doubt about its covalency (from the AIM theory point of view). When  $H_c < 0$ , we have an H-bond or van der Waals interaction while  $H_c > 0$  returns to bonds with a covalent in character. Also, the  $-G_c/V_c$  ratio specifies the nature of interactions. Hence, the value of  $-G_c/V_c$  can indicate the character of interactions which is covalent or non-covalent in their natures. If such a ratio is greater than one, ( $-G_c/V_c > 1$ ), the interaction is non-covalency.

Table 4. Unscaled vibrational frequencies ( $\nu$ ,  $\text{cm}^{-1}$ ) of C=C and C=N in free PZ and their [PZ:HOX] complexes with the frequency shifts ( $\Delta\nu$ ,  $\text{cm}^{-1}$ ).

Compound	$\nu_{\text{C=C}}$	$\Delta\nu_{\text{C=C}}$	$\nu_{\text{C=N}}$ (Asym)	$\Delta\nu_{\text{C=N}}$ (Asym)	$\nu_{\text{C=N}}$ (Sym)	$\Delta\nu_{\text{C=N}}$ (Sym)
PZ	1603		1549		1340	
PZ:HOF-A-HB	1614	11	1554	5	1351	11
PZ:HOCl-A-HB	1613	10	1554	5	1351	11
PZ:HOBBr-A-HB	1613	10	1554	5	1352	12
PZ:HOI-A-HB	1612	9	1554	5	1354	14
PZ:HOF-A-XB	1603	0	1548	-1	1340	0
PZ:HOCl-A-XB	1605	2	1553	4	1348	8
PZ:HOBBr-A-XB	1606	3	1554	5	1352	12
PZ:HOI-A-XB	1607	4	1552	3	1356	16
PZ:HOCl-B	1599	-4	1548	-1	1346	6
PZ:HOBBr-B	1596	-7	1547	-2	1347	7
PZ:HOI-B	1594	-9	1546	-3	1347	7

Table 5. Topological parameters for the complexes between PZ and hypohalous acids (HOX, X= F, Cl, Br and I) at the MP2/6-311++G(2d,2p) level.

Complex	bcp	$\rho$	$\nabla^2$	-Gc	Vc	-Gc/Vc	Hc
PZ:HOF-A-HB	N...H	0.0447	0.0961	-0.0308	-0.0376	0.8194	-0.0068
PZ:HOCl-A-HB	N...H	0.0468	0.0972	-0.0322	-0.0401	0.8029	-0.0079
PZ:HOBBr-A-HB	N...H	0.0457	0.0968	-0.0315	-0.0388	0.8115	-0.0073
PZ:HOI-A-HB	N...H	0.0455	0.0970	-0.0315	-0.0387	0.8131	-0.0072
PZ:HOF-A-XB	N...F	0.0057	0.0250	-0.0054	-0.0046	1.1791	0.0008
PZ:HOCl-A-XB	N...Cl	0.0308	0.1039	-0.0248	-0.0236	1.0513	0.0012
PZ:HOBBr-A-XB	N...Br	0.0379	0.1112	-0.0288	-0.0299	0.9648	-0.0011
PZ:HOI-A-XB	N...I	0.0425	0.1072	-0.0310	-0.0352	0.8804	-0.0042
PZ:HOCl-B	C...Cl	0.0104	0.0369	0.0076	-0.0059	1.2836	0.0017
PZ:HOBBr-B	C...Br	0.0121	0.0387	0.0083	-0.0070	1.1903	0.0013
PZ:HOI-B	C...I	0.0141	0.0417	0.0093	-0.0081	1.1437	0.0012

If ( $0.5 < -G_c/V_c < 1$ ), the interaction is partly covalent character in its nature and if it is less than 0.5 ( $-G_c/V_c < 0.5$ ), the interaction is covalency. The molecular graphs and values of topological parameters for each intermolecular BCPs of complexes are presented in Table 5.

The values of electron densities at BCP for the  $N\cdots X$  in PZ:HOX-A-XB and  $\pi\cdots X$  in PZ:HOX-B becomes greater with an increase in X atomic mass, which is in accordance with the changes of stabilization energy and confirming the stronger halogen bond. It also concludes that the halogen bond in PZ:HOX-A-XB was stronger than that in PZ:HOX-B. The electron density at BCP of the  $N\cdots H$  in PZ:HOX-A-HB becomes smaller with the increase of X atomic number, exception in PZ:HOF-A-HB which has minimum electron density. The PZ:HOX-A-HB complexes have  $\nabla^2\rho_{\text{BCP}} > 0$ ,  $H_C < 0$ , and  $-G_C/V_C \approx 0.81$  thus they are hydrogen bonds with a weak covalency in their nature. In the PZ:HOX-A-XB complexes, the PZ:HOF-A-XB and PZ:HOCl-A-XB have  $\nabla^2\rho_{\text{BCP}} > 0$ ,  $H_C > 0$ , and  $-G_C/V_C > 1$  as result they have a purely closed shell XB, whereas  $\nabla^2\rho_{\text{BCP}} > 0$ ,  $H_C < 0$ , and  $-G_C/V_C \approx 0.9$  corresponding to PZ:HOBBr-A-XB and PZ:HOI-A-XB indicate that they have XB interactions with partially covalent character in their nature. Regards  $\nabla^2\rho_{\text{BCP}} > 0$ ,  $H_C > 0$ , and  $-G_C/V_C > 1$  for PZ:HOX-B complexes, therefore they show non-covalent XB interaction with purely closed shell characteristics. In the PZ:HOX-A-HB complexes (X = Cl, Br and I), the  $N\cdots H$  bond distances become larger with the increase of the X atomic mass, which it corresponds to the weaker  $N\cdots H$  hydrogen bond, and this is consistent with the values of electron densities at the  $N\cdots H$ BCPs ( $\rho_{\text{H}\cdots\text{C}}$ ) as well as with their vibrational frequencies ( $\nu_{\text{N}\cdots\text{H}}$ ). Figure 5 shows the linear correlation between the electron densities ( $\rho$ ) at the  $N\cdots H$  BCPs with the stabilization energies ( $SE^{\text{corr}}$ ) and interatomic  $N\cdots H$  distances in PZ:HOX-A-HB complexes.

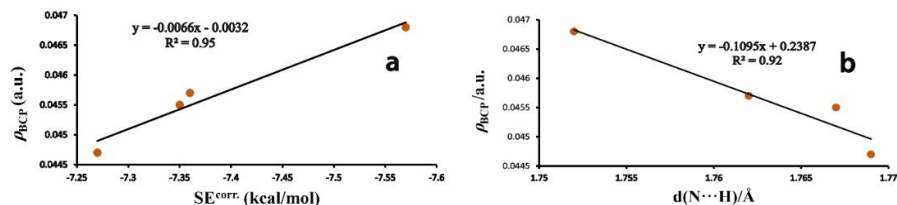


Figure 5. Relationship between the electron densities at the  $N\cdots H$  BCPs with the interaction energies (a) and  $N\cdots H$  distances (b) in PZ:HOX-A-HB complexes.

## NBO ANALYSES

To detailed analysis of the charge-transfers, we performed natural bond orbital (NBO) calculations [45] for the minima found on the studied HB and XB complexes (Table 6). The PZ:HOX-A complexes were associated with an orbital interaction between the lone pairs in the electron donor ( $lp_N$ ) and the antibonding orbitals ( $\sigma^*_{\text{O-H}}$  and  $\sigma^*_{\text{O-X}}$ ) in the electron acceptor molecule. While in the PZ:HOX-B, complex formations are associated with an orbital interaction between the  $\pi$  bond in the electron donor ( $\pi_{\text{C=C}}$ ) and the antibonding orbital in the electron acceptor ( $\sigma^*_{\text{O-X}}$ ) as well as  $lp_X$  in HOX as electron donor and  $\pi^*_{\text{C=C}}$  in PZ as electron acceptor. The NBO analysis stresses the role of intermolecular orbital interaction in the complex, particularly charge transfer. The second-order perturbation energy ( $E^2$ ) can be taken as an index to judge the strength of intermolecular interactions. Table 5 shows the main orbital interactions corresponding to each type of interactions which is present in the complexes.

The large  $lp_N \rightarrow \sigma^*_{\text{O-H}}$  and  $lp_N \rightarrow \sigma^*_{\text{O-X}}$  (X = Cl, Br and I) orbital interactions were observed in the PZ:HOX-A complexes, which can be used to explain the elongation and red shift of their O-H and O-X bonds. The  $lp_N \rightarrow \sigma^*_{\text{O-H}}$  orbital interaction becomes smaller with increasing X atomic number in HB complexes and give weaker  $N\cdots H$  bonds. Whereas in XB types the  $lp_N \rightarrow \sigma^*_{\text{O-X}}$  orbital interaction raised as the X atomic number increases and lead to stronger  $N\cdots X$  halogen bonds. The  $lp_X \rightarrow \pi^*_{\text{C=C}}$  and  $\pi_{\text{C=C}} \rightarrow \pi^*_{\text{O-X}}$  (X = Cl, Br and I) orbital interactions in



the PZ:HOX-B complexes becomes larger with increasing of X atomic number. This can be responsible for the elongation and red shift of the O–H and O–X bonds. In all complexes, the charge transfers are in agreement with the stabilization energies. According to Table 6, with an increase in X atomic number, the charge transfer decreases in the HB, whereas it increases in the XB complexes.

Table 6. Second-order perturbation energies ( $E_1^{2^{\circ}}$ , kcal mol<sup>-1</sup>), charge transfer (CT, e) of the PZ-HOX complexes at the MP2/6-311++G(2d,2p) level.

Complex	CT	$E_1^{2^{\circ}}$	$E_2^{2^{\circ}}$
PZ:HOF-A-HB	0.0394	29.38	
PZ:HOCl-A-HB	0.0393	29.91	
PZ:HOBBr-A-HB	0.0383	28.31	
PZ:HOI-A-HB	0.0324	25.16	
PZ:HOF-A-XB	0.0023	0.11	0.30
PZ:HOCl-A-XB	0.0287	12.69	
PZ:HOBBr-A-XB	0.0500	22.66	
PZ:HOI-A-XB	0.0587	34.37	
PZ:HOCl-B	0.0029	2.96	0.78
PZ:HOBBr-B	0.0083	4.91	1.32
PZ:HOI-B	0.0126	6.91	2.15

<sup>a</sup> $E_1$  corresponds to  $lp_N \rightarrow \sigma^*_{O-H}$  orbital interaction in PZ:HOX-A-HB,  $lp_N \rightarrow \sigma^*_{O-X}$  orbital interaction in PZ:HOX-A-XB and  $\sigma_{C-C} \rightarrow \sigma^*_{O-X}$  orbital interaction in PZ:HOX-B.

<sup>b</sup> $E_2$  corresponds to  $lp_F \rightarrow \sigma^*_{C-H}$  orbital interaction in PZ:HOF-B and  $lp_X \rightarrow \sigma^*_{C-C}$  orbital interaction in PZ:HOX-B.

## CONCLUSIONS

Complex pairing of pyrazine with hypohalous acids carried out via HB and XB interactions. Except to HOI, in other HOX molecules HB interactions are stronger than the XB. The HB complexes show blue and red shift for the X–O and H–O stretching frequencies, respectively. In the XB complexes the X–O stretching frequencies had red shift while the H–O stretching frequencies displayed blue shift in PZ:HOX-A-XB but red shift in PZ:HOX-B. The C=N and C=C bonds of PZ in PZ:HOX-A systems show blue shift with respect to free PZ molecule. In PZ:HOX-B the  $\nu_{C=N(Asym)}$  and  $\nu_{C=C}$  show small red shift while  $\nu_{C=N(Sym)}$  shows blue shift with complexation.

## ACKNOWLEDGEMENTS

We are grateful to the Department of Chemistry, Lorestan University, for providing laboratory facilities and financial support.

## REFERENCES

1. Wu, J.; Wang, F.-M.; Liu, J.-Q.; Chen, J.-X.; Wu, J.-M.; Li, K.-B.; Wei, Y.; Li Q.-L. Two new 1D coordination polymers: syntheses, structures and properties. *Bull. Chem. Soc. Ethiop.* **2014**, 28, 415-422.
2. Jeffrey, G.A. *An Introduction to Hydrogen Bonding*, Oxford University Press: New York; **1997**.
3. Zhang, X.-C.; Liu, B. Two Zn and Hg bromide salts based on 1-ethyl-3-methyl imidazolium ionic liquid: Ionothermal synthesis, structures and supramolecular organization. *Bull. Chem. Soc. Ethiop.* **2012**, 26, 407-414.

4. Assefa, Z.; Gore, S.B. Structural and spectroscopic studies of 2,9-dimethyl-1,10-phenanthroline cation(dph) with chloride, triflate and gold dicyanide anions. The role of h-bonding in molecular recognition and enhancement of  $\pi$ - $\pi$  stacking. *Chem. Soc. Ethiop.* **2016**, 30, 231-239.
5. Czyznikowska Z. On the importance of electrostatics in stabilization of stacked guanine-adenine complexes appearing in B-DNA crystals. *J. Mol. Struct. THEOCHEM* **2009**, 895, 161-167.
6. Scheiner S. Detailed comparison of the pnictogen bond with chalcogen, halogen, and hydrogen bonds. *Int. J. Quantum Chem.* **2013**, 113, 1609-1620.
7. Auffinger, P.; Hays F.A.; Westhof, E.; Ho, P.S. Halogen bonds in biological molecules. *Proc. Natl. Acad. Sci. U.S.A.* **2004**, 101, 16789-16794.
8. Voth, A.R.; Hays, F.A.; Ho, P.S. Directing macromolecular conformation through halogen bonds. *Proc. Natl. Acad. Sci. U.S.A.* **2004**, 104, 6188-6193.
9. Li, Q.; Xu, X.; Liu, T.; Jing, B.; Li, W.; Cheng, J.; Gong, B.; Sun, J. Competition between hydrogen bond and halogen bond in complexes of formaldehyde with hypohalous acids. *Phys. Chem. Chem. Phys.* **2010**, 12, 6837-6843.
10. Battistutta, R.; Mazzorana, M.; Sarno, S.; Kazimierczuk, Z.; Zanotti, G.; Pinna, L.A. Inspecting the structure-activity relationship of protein kinase CK2 inhibitors derived from tetrabromo-benzimidazole. *Chem. Biol.* **2005**, 12, 1211-1219.
11. Metrangolo, P.; Neukirch, H.; Pilati, T.; Resnati, G. Halogen bonding based recognition processes: A world parallel to hydrogen bonding. *Acc. Chem. Res.* **2005**, 38, 386-395.
12. Politzer, P.; Lane, P.; Concha, M.C.; Ma, Y.; Murria, J.S. An overview of halogen bonding. *J. Mol. Model.* **2007**, 13, 305-311.
13. Palusiak, M.; Grabowski, S.J. Do intramolecular halogen bonds exist? Ab initio calculations and crystal structures' evidences. *Struct. Chem.* **2008**, 19, 5-11.
14. Lu, Y.X.; Zou, J.W.; Wang, Y.H.; Jiang, Y.J.; Yu, Q.S. Ab initio investigation of the complexes between bromobenzene and several electron donors: some insights into the magnitude and nature of halogen bonding interactions. *J. Phys. Chem. A* **2007**, 111, 10781-10788.
15. Gilday, L.C.; Lang, T.; Caballero, A.; Costa, P.J.; Felix, V.; Beer, P.D. A catenane assembled through a single charge-assisted halogen bond. *Angew. Chem. Int. Ed.* **2013**, 52, 4356-4360.
16. Jentsch, A.V.; Matile, S. Transmembrane halogen-bonding cascades. *J. Am. Chem. Soc.* **2013**, 135, 5302-5303.
17. Ormond-Prout, J.E.; Smart, P.; Brammer, L. Cyanometallates as halogen bond acceptors. *Cryst. Growth Des.* **2012**, 12, 205-216.
18. Solimannejad, M.; Pejov, L. Computational investigation of the weakly bound dimers  $\text{HOX}\cdots\text{SO}_3$  (X = F, Cl, Br). *J. Phys. Chem. A* **2005**, 109, 825-831.
19. Wu, W.; Zeng, Y.; Li, X.; Zhang, X.; Zheng, S.; Meng, L. Interplay between halogen bonds and hydrogen bonds in  $\text{OH}/\text{SH}\cdots\text{HOX}\cdots\text{HY}$  (X = Cl, Br; Y = F, Cl, Br) complexes. *J. Mol. Model.* **2013**, 19, 1069-1071.
20. Zeng, Y.; Wu, W.; Li, X.; Zheng, S.; Meng, L. Influence of the  $\text{Li}\cdots\pi$  interaction on the  $\text{H}/\text{X}\cdots\pi$  interactions in  $\text{HOLi}\cdots\text{C}_6\text{H}\cdots\text{HOX}/\text{XOH}$  (X = F, Cl, Br, I) complexes. *ChemPhysChem* **2013**, 14, 1591-1600.
21. Solimannejad, M.; Alkorta, I.; Elguero, J. Stabilities and properties of  $\text{O}_3\text{-HOCl}$  complexes: A computational study. *Chem. Phys. Lett.* **2007**, 449, 23-27.
22. Tang, Q.; Guo, Z.; Li, Q. A quantum chemical study of the structures, stability, and spectroscopy of halogen- and hydrogen-bonded complexes between cyanoacetaldehyde and hypochlorous acids. *Spectrochim. Acta Mol. Biomol. Spectrosc.* **2014**, 121, 157-163.

23. Yuan, K.; Liu, Y.Z.; Zhu, Y.C.; Zhang, J.; Zhang, J.Y. Structures and properties of halogen bond and hydrogen bond formed between CH<sub>3</sub>SH and HOCl. *Acta Chin. Sin.* **2009**, *67*, 499-506.
24. Zhao, Q.; Feng, D.; Sun, Y.; Hao, J.; Cai, Z. Theoretical investigations of the H... $\pi$  and X (X=F, Cl, Br, I)... $\pi$  complexes between hypohalous acids and benzene. *J. Mol. Model.* **2012**, *17*, 1935-1939.
25. Zabaradsti, A.; Kakanejadifard, A.; Ghasemian, M. Theoretical study of molecular interactions of phosphorus ylide with hypohalous acids HOF, HOCl and HOBr. *Comput. Theor. Chem.* **2012**, 989, 1-6.
26. Solomon, S.; Garsia, R.R.; Rowland, F.S.; Weubles, D.J. On the depletion of Antarctic ozone. *Nature* **1986**, *321*, 755-758.
27. Francisco, J.S.; Sander, S.P. Structure and thermochemistry of hydrochlorous acid, HOCl. *J. Chem. Phys.* **1993**, *99*, 6219-6220.
28. McGrath, M.P.; Rowland, F.S. A comparative study of the diatomic halogen oxides in their ground electronic states. *J. Phys. Chem.* **1996**, *100*, 4815-4822.
29. Thomas, E. Myeloperoxidase, hydrogen peroxide, chloride antimicrobial system: Nitrogen-chlorine derivatives of bacterial components in bactericidal action against *Escherichia coli*. *Infect. Immun.* **1979**, *23*, 522-531.
30. Poll, W.; Pawelke, G.; Mootz, D.; Appelman, E.H. The crystal structure of hypofluorous acid: Chain formation by O-H...O hydrogen bonds. *Angew. Chem. Int. Ed. Engl.* **1988**, *27*, 392-393.
31. Rozen, S.; Mishani, E.; Kol, M. A novel electrophilic methoxylation (with a little help from fluorine). *J. Am. Chem. Soc.* **1992**, *114*, 7643-7645.
32. Appelman, E.H. Nonexistent compounds. Two case histories. *Acc. Chem. Res.* **1973**, *6*, 113-117.
33. Glukhovstev, M.N.; Pross, A.; Radom, L. Acidities, proton affinities, and other thermochemical properties of hypohalous acids HOX (X = F-I): A high-level computational study. *J. Phys. Chem.* **1996**, *100*, 3498-3503.
34. Panek, J.J.; Berski, S. Symmetry-adapted perturbation theory study of dimers and water complexes of hypohalous acids HOF, HOCl and HOBr. *Chem. Phys. Lett.* **2008**, *467*, 41-45.
35. Roohi, H.; Nowroozi, A.; Eshghi, F. The gas phase hydrogen-bonded dimers of HOCl: A high-level quantum chemical study. *Int. J. Quantum. Chem.* **2010**, *110*, 1489-1499.
36. Zhang, Z.; Shen, J.; Jin, N.; Chen, L.; Yang, Z. Possible dimers of hypochlorous acid (HOCl) arising from hydrogen- and halogen-bond interactions. *Comput. Theor. Chem.* **2012**, *999*, 48-54.
37. Shen, T.; Huang, Z.; Guo, L.; Wang, H. An ab initio study on the insertion of radon atoms into hypohalous acids. *Inorg. Chim. Acta* **2012**, *386*, 68-72.
38. Solimannejad, M. Computational investigation of the weakly bound dimers HOX...SO<sub>3</sub> (X = F, Cl, Br). *J. Phys. Chem. A* **2005**, *109*, 825-831.
39. Zabardasti, A.; Kakanejadifard, A.; Goudarziafshar, H.; Salehnassaj, M.; Zohrehband, Z.; Jaberansari, F.; Solimannejad, M. Theoretical study of hydrogen and halogen bond interactions of methylphosphines with hypohalous acids. *Comput. Theor. Chem.* **2013**, 1014, 1-7.
40. Meher, C.P.; Rao, A.M.; Omar, M. Piperazine-pyrazine and their multiple biological activities. *Asian J. Pharm. Sci. Res.* **2013**, *3*, 43-60.
41. Moller, C.; Plesset, M.S. Note on an approximation treatment for many-electron systems. *Phys. Rev.* **1934**, *46*, 618-622.
42. Frisch, M.J.; Pople, J.A.; Binkley, J.S. Self-consistent molecular orbital methods 25. Supplementary functions for Gaussian basis sets. *J. Chem. Phys.* **1984**, *80*, 3265-3269.

43. Weigend, F.; Ahlrichs, R. Balanced basis sets of split valence, triple zeta valence and quadruple zeta valence quality for H to Rn: Design and assessment of accuracy. *Phys. Chem. Chem. Phys.* **2005**, *7*, 3297-3305.
44. Boys, S.F.; Bernardi, F. The calculation of small molecular interactions by the differences of separate total energies. Some procedures with reduced errors. *Mol. Phys.* **1970**, *19*, 553-566.
45. Reed, A.E.; Curtiss, L.A.; Weinhold, F. Intermolecular interactions from a natural bond orbital, donor-acceptor viewpoint. *Chem. Rev.* **1988**, *88*, 899-926.
46. Frisch, M.J.; Trucks, G.W.; Schlegel, H.B.; Scuseria, G.E.; Robb, M.A.; Cheeseman, J.R.; Montgomery, J.A.; Vreven, Jr. T.; Kudin, K.N.; Burant, J.C.; Millam, J.M.; Iyengar, S.S.; Tomasi, J.; Barone, V.; Mennucci, B.; Cossi, M.; Scalmani, G.; Rega, N.; Petersson, G.A.; Nakatsuji, H.; Hada, M.; Ehara, M.; Yota, K.; Fukuda, R.; Hasegawa, J.; Ishida, M.; Nakajima, T.; Honda, Y.; Kitao, O.; Nakai, H.; Klene, M.; Li, X.; Knox, J.E.; Hratchian, H.P.; Cross, J.B.; Adamo, C.; Jaramillo, J.; Gomperts, R.; Stratmann, R.E.; Yazyev, O.; Austin, A.J.; Cammi, R.; Pomelli, C.; Ochterski, J.W.; Ayala, P.Y.; Morokuma, K.; Voth, G. A.; Salvador, P.; Dannenberg, J.J.; Zakrzewski, V.G.; Dapprich, S.; Daniels, A.D.; Strain, M.C.; Farkas, O.; Malick, D.K.; Rabuck, A.D.; Raghavachari, K.; Foresman, J.B.; Ortiz, J.V.; Cui, Q.; Baboul, A.G.; Clifford, S.; Cioslowski, J.; Stefanov, B.B.; Liu, G.; Liashenko, A.; Piskorz, P.; Komaromi, I.; Martin, R.L.; Fox, D.J.; Keith, T.; Al-Laham, M.A.; Peng, C.Y.; Nanayakkara, A.; Challacombe, M.; Gill, P.M.W.; Johnson, B.; Chen, W.; Wong, M.W.; Gonzalez, C.; Pople, J.A. *Gaussian 03, Revision B.01*, Gaussian, Inc.: Pittsburgh, PA; **2003**.
47. Bader, R.F.W. *Atoms in Molecules: A Quantum Theory*, Oxford University Press: Oxford; **1990**.
48. An, X.; Zhuo, H.; Wang, Y.; Li, Q. Competition between hydrogen bonds and halogen bonds in complexes of formamidine and hypohalous acids. *J. Mol. Model.* **2013**, *19*, 4529-4535.
49. Berski, S.; Silvi, B.; Latajka, Z.; Leszczynski, J. Bonding in hypohalous acids HOX (X = F, Cl, Br, and I) from the topological analysis of the electron localization function. *J. Chem. Phys.* **1999**, *111*, 2542-2555.
50. Torii, H.; Yoshida, M. Properties of halogen atoms for representing intermolecular electrostatic interactions related to halogen bonding and their substituent effects. *J. Comput. Chem.* **2010**, *31*, 107-116.